Calculation of ion-surface collisions for a wide range of scattering geometries

M. C. Torralba,[1] P. G. Bolcatto,[2,3] and E. C. Goldberg[1,2]
[1]*Instituto de Desarrollo Tecnológico para la Industria Química (CONICET-UNL) cc91, 3000 Santa Fe, Argentina*
[2]*Facultad de Ingeniería Química, Santiago del Estero 2829 3000 Santa Fe, Argentina*
[3]*Facultad de Humanidades y Ciencias, Ciudad Universitaria Paraje El Pozo, 3000 Santa Fe, Argentina*
(Received 27 December 2002; revised manuscript received 9 April 2003; published 14 August 2003)

A theoretical calculation that accounts for a fairly complete description of the resonant charge-exchange process occuring in the H^+ scattering by metal surfaces is presented. Realistic trajectories defined by the binary collision model are considered. The interaction with nuclei and electrons of the all surface atoms that the projectile can see along its trajectory is calculated within a mean-field approximation, and in this form the contributions of the short-range interaction terms to the energy level shift are well contemplated. The long-range contributions and the motion of the projectile respect to the surface reference frame are also taken into account to define the level shift. All these ingredients are incorporated into a quantum mechanical description of the time evolution. The negative ion fractions calculated in this form show an excellent agreement with the experimental data for three different incoming energies and for a wide range of exit angles.

DOI: 10.1103/PhysRevB.68.075406 PACS number(s): 73.20.Hb, 73.20.At, 71.10.−w

I. INTRODUCTION

In ion-surface collisions and taking the scattering angle as a relevant parameter we can distinguish three regimes: (i) a large scattering angle that in the backscattering condition involves almost normal collisions; (ii) a small scattering angle, or the grazing collisions regime; and (iii) the intermediate scattering angle involving nonspecular collisions in general.

The large angle regime in the backscattering condition has been analyzed for many different projectile-target combinations.[1–5] The theoretical approaches based on the interaction between the projectile and only the scatterer atom at the surface are able to reproduce the experimental trends.[6–8] On the other hand, grazing-angle collisions[9,10] have been described by using the resonance properties of the projectile level in front of the surface, position and width, and justifying a semiclassical rate equation for the calculation of the projectile-state population based on the broadening of the electron distribution caused by the parallel component of the velocity.[11,12]

The interest now resides in the search of an appropriate theoretical description of collisions occurring between these two limit conditions and this is the aim of the present work. Here the collisions with small impact parameter are expected to be important, and then, a quantitative approach in this case requires a good description of the surface, including both, the electronic and crystallographic structures. The projectile interacting with the nuclei and electrons of the surface atoms along a trajectory that is determined by the binary collision with one atom at the surface, is a good approximation to the single scattering process. This picture points to the opposite limit of the grazing collision regime where scattering is dominated by large atom-surface distances and a jellium description is possible.

Maazouz and co-workers[13,14] have measured the H^- formation in collisions of H^- and H^+ ions of 1,2, and 4 keV against Al surfaces for a scattering angle of 38°, being the emerging ion fractions investigated in an exit angular range covering from 2° to 35° respect to the surface plane. As the measurements performed with both H^- and H^+ beams give practically the same negative ion fractions, it is possible to state that the memory of the incident-ion charge is lost due to a very efficient resonant neutralization in the incoming trajectory.

Several theoretical approaches[12,15,16] have been applied to reproduce these experimental data. All of them use the semiclassical rate equation which accounts only for the second half of the collision when the atom (ion) leaves the surface, and the initial charge state in this case is a parameter that has to be introduced in the calculation. For large values of the perpendicular component of velocity or large exit angles, the results are different depending on the initial charge state assumed (H^0 or H^-), and it is found a better agreement with experiment for H^0 as the initial charge condition. This is discussed in terms of the collisions with surface atoms at small impact parameters occurring in the scattering with rather large exit angles. The authors say that in such violent collisions one can expect that any H^- formed in the incoming trajectory would lose its outer electron, justifying in this form the neutral initial condition. Finally, two important conclusion from these works are that for this large range of collision angles: (i) a better description of the surface, including its crystallographic structure; and (ii) a quantum mechanical calculation of the charge transfer process that accounts for the violent collisions more properly that the semiclassical rate equations are required.

In this direction, Merino *et al.*[16] take into account the short-range interactions for calculating the position and width of the projectile level. The starting point is a many-body Hamiltonian written within a second quantization language where the terms involving four different state-indexes are neglected. Then, an effective Hamiltonian is obtained by performing a local density-like-approach to the two-electron terms; and the ionization and affinity levels of the projectile are calculated from total energy differences. The negative ion formation in collisions of 1–4 keV positive hydrogen ions

with Al (100) surface is then calculated in a very similar way to that in Ref. 12. In the case of positive hydrogen fractions, they discuss the necessity of a quantum mechanical calculation because of the finite bandwidth effects.[17] However, in any case they take into account realistic trajectories along the surface accordingly with the experimental scattering geometries; they consider normal trajectories that include the interaction with the nearest neighbor surface atoms (one atom in the top case and four in the center one).

In the present work the projectile trajectory is defined by the binary collision with one atom at the surface, but the electronic processes involve the interaction with *all* the surface atoms inside a sphere of radius equal to 11 a.u. (neighbor-atom sphere) centered at the projectile position in each point of the trajectory. This picture assumes that the elastic processes respond to a binary model while the inelastic processes do not. The energy level of the projectile and the hopping with the orbitals of each surface atom are calculated by using the bond-pair model[18] that is an *ab initio* approach to the atom-surface interaction solved within a Hartee-Fock approximation to the many-body problem. The bond-pair model allows to recover the Anderson-Newns Hamiltonian where the on-site energy and hopping terms are defined up from both the local density of states of the surface and the atomic properties of the one- and two-electron interactions. In Ref. 18 the interaction energy as well as the width and shift of the adatom level for H adsorption on metal surfaces were calculated by using this model calculation, and the long-range interactions were included through an image potential that resumes the collective effects involved in the surface response. In this form, it is obtained a good description of the interaction for a large range of atom-surface distances that compares quite well with earlier approaches.[19] The same proposals are used in this work for describing the dynamical collision process in which the time-dependence of the Hamiltonian terms comes from the classical atom trajectory. The energy and hopping terms of the time-dependent Hamiltonian correspond to those from the adiabatic atom-surface interaction without charge transfer. The large distance behavior of the projectile energy level is corrected by the image potential contribution; and the dynamical effects related with the Galilean transformation that takes into account the projectile motion respect to the surface, are considered only in the energy shift associated with the electron kinetic energy. The time evolution of the interacting system within a quantum-mechanical description is obtained by using the Green's function method introduced by Keldysh.[20] Therefore, the calculation presented in this work takes into account the short-range interactions between the projectile and the surface atoms along the trajectory described in a realistic way, the long-range interactions due to the presence of a metal surface, and, finally, the energy shift of the projectile level due to its motion in the reference frame fixed at the surface. This is a very complete and detailed description of the collisional process that allows for an analysis of each isolated effect, and also allows to infer the relevance of the time interferences along the whole trajectory in the charge transfer process. The excellent agreement of our results with the experimental ones of Maazouz and co-workers.[13,14] is encouraging for future applications of this model calculation to a great variety of atom-surface collisional systems.

The work is organized as follows. In Sec. II there is a detailed description of the theoretical aspects, while Sec. III is devoted to a discussion of the results. Finally we present concluding remarks in Sec. IV.

II. THEORY

In the case of H^+ colliding with an Al surface, the ionization level (-13.6 eV) is resonant with the valence band and a practically total neutralization is expected in the incoming trajectory. Then, the H^- formation from neutral incoming atoms provides a good approximation to the H^+/Al collision. A correct treatment of this problem requires one to introduce the intra-atomic Coulomb repulsion term U. The statistical spin factors used in the rate equation approach,[21] and justified from an infinite-U limit approximation,[22] do not apply to a quantum time-dependent formalism like the one developed in this work. On the other hand, these spin factors are very important in the case of a two-fold degenerate state of the incoming particle. But in the H^- formation from neutral incoming atoms, a first order perturbative treatment of the correlation term given by the time-dependent Hartree-Fock approximation results to be appropriate[23]. Taking into account the energy locations of the ionization and affinity levels with respect to the Fermi level, and the neutral H as the incoming particle, small changes of the initial spin-state occupations are expected. Then, to freeze the occupation of the first spin state to its initial value ($\langle n_\uparrow \rangle = 1$), and only to consider the variations of the average occupation of the second spin state ($\langle n_\downarrow \rangle$) in the presence of the mean field provided by the first electron, is finally a rather good approximation to the H^- formation in the H/Al collision.[23]

In this spinless approach, the expression of the Hamiltonian is

$$H(t) = \sum_{\mathbf{k}} \varepsilon_{\mathbf{k}} \hat{n}_{\mathbf{k}} + \sum_{c} \varepsilon_c \hat{n}_c + E_a(t)\hat{n}_a + \sum_{\mathbf{k}} [V_{a\mathbf{k}}(t)\hat{c}_a^+ \hat{c}_{\mathbf{k}} + \text{H.c.}] + \sum_{c} [V_{ac}(t)\hat{c}_a^+ \hat{c}_c + \text{H.c.}], \quad (1)$$

where the index a refers to the active state localized on the projectile atom with energy $E_a(t)$, while the indexes $\mathbf{k}$ and c refer to the valence-band and core-band states of the solid respectively, with energies $\varepsilon_{\mathbf{k}}$ and ε_c; being $V_{a\mathbf{k}}(t)$ and $V_{ac}(t)$ the respective hopping parameters. The time dependence of the parameters comes from the classical trajectory $\vec{R} = \vec{R}(t)$.

A. Quantum mechanical calculation of the charge exchange

In the spinless approximation $\langle \hat{n}_a(t) \rangle$ gives the probability that the projectile state is occupied at the time value t. The other possibility for the projectile state is the empty state with probability given by $1 - \langle \hat{n}_a(t) \rangle$. The average occupation number is calculated by using the following Green function:

$$F_{aa}(t,t') = i\langle [c_a^+(t'), c_a(t)]\rangle, \tag{2}$$

where [ ] indicates the commutator, and $\langle \hat{n}_a(t)\rangle$ is obtained from this Green function evaluated at equal time values:

$$-iF_{aa}(t',t') = 2\langle \hat{n}_a(t')\rangle - 1. \tag{3}$$

The $F_{aa}(t,t')$ function is calculated by solving its equation of motion:

$$\frac{dF_{aa}(t,t')}{dt} = i\left\langle \left[c_a^+(t'), \frac{dc_a(t)}{dt}\right]\right\rangle = i\langle [c_a^+(t'), -i[H(t), c_a(t)]]\rangle. \tag{4}$$

Accordingly with expression (1) for the Hamiltonian, Eq. (4) results to be

$$i\frac{dF_{aa}(t,t')}{dt} = E_a(t)F_{aa}(t,t') + \sum_{\mathbf{k}} V_{a\mathbf{k}}(t)F_{\mathbf{k}a}(t,t') + \sum_c V_{ac}(t)F_{ca}(t,t'). \tag{5}$$

The new functions $F_{qa}(t,t')$ (with $q=\mathbf{k},c$) are

$$F_{qa}(t,t') = i\langle [c_a^+(t'), c_q(t)]\rangle,$$

their equations of motion being

$$idF_{qa}(t,t')/dt = \varepsilon_q F_{qa}(t,t') + V_{qa}(t)F_{aa}(t,t'). \tag{6}$$

The result obtained by introducing the phase transformation $F_{qa}(t,t') = f_{qa}(t,t')\exp[-i\varepsilon_q(t-t')]$ and integrating Eq. (6), is then replaced in Eq. (5). In this form, the equation of motion for $F_{aa}(t,t')$ is

$$i\frac{dF_{aa}(t,t')}{dt} = E_a(t)F_{aa}(t,t') + \int_{t_0}^{t} d\tau(\Sigma_{vb}^r(t,\tau) + \Sigma_{core}^r(t,\tau))F_{aa}(\tau,t') + \sum_k V_{a\mathbf{k}}(t)\exp[-i\varepsilon_{\mathbf{k}}(t-t_0)]F_{\mathbf{k}a}(t_0,t') + \sum_c V_{ac}(t)\exp[-i\varepsilon_c(t-t_0)]F_{ca}(t_0,t'), \tag{7}$$

where t_0 is the initial time for the collisional process, and the retarded self-energies $\Sigma_{vb}^r(t,\tau)$ and $\Sigma_{core}^r(t,\tau)$ are defined as

$$\Sigma_X^r(t,\tau) = -i\Theta(t-\tau)\sum_q V_{aq}(t)V_{qa}(\tau)\exp[i\varepsilon_q(t-\tau)], \tag{8}$$

with $q=\mathbf{k}$ for $X=vb$, and $q=c$ for $X=$core.

The $F_{qa}(t_0,t')$ functions are still required to solve Eq. (7). They can be determined by using the advanced Green functions $G_{qa}(t,t') = i\Theta(t'-t)\langle\{c_a^+(t'), c_q(t)\}\rangle$, with { } indicating the anticommutator.

There exists the following relation between the F and G functions at $t=t_0$, provided the occupation of the q state is either 0 or 1 at this time:

$$F_{qa}(t_0,t') = (2n_q - 1)G_{qa}(t_0,t'),$$

with $n_q = 1(0)$ if the q state is occupied (empty) at the time t_0. The motion equations for the G functions are obtained in a similar way as that for the F functions. The final results are

$$i\frac{dF_{aa}(t,t')}{dt} = E_a(t)F_{aa}(t,t') + \int_{t_0}^{t} d\tau(\Sigma_{vb}^r(t,\tau) + \Sigma_{core}^r(t,\tau))F_{aa}(\tau,t') + \int_{t_0}^{t'} d\tau(\Omega_{vb}(t,\tau) + \Omega_{core}(t,\tau))G_{aa}(\tau,t') \tag{9}$$

and

$$i\frac{dG_{aa}(t,t')}{dt} = E_a(t)G_{aa}(t,t') + \int_{t}^{t'} d\tau[\Sigma_{vb}^a(t,\tau) + \Sigma_{core}^a(t,\tau)]G_{aa}(\tau,t'), \tag{10}$$

where the new self-energies are defined as follows:

$$\Sigma_X^a(t,\tau) = [\Sigma_X^r(\tau,t)]^*,$$

$$\Omega_X(t,\tau) = i\sum_q (2n_q - 1)V_{aq}(t)V_{qa}(\tau)\exp[i\varepsilon_q(t-\tau)]. \tag{11}$$

Equations. (9), (10) and (3) finally allow for the calculation of the average charge state of the projectile given by $\langle \hat{n}_a(t)\rangle$. In the case of self-energies and a projectile energy level that are not dependent on $\langle \hat{n}_a(t)\rangle$, the integration of these equations is performed by considering the time value t' fixed at the final time for the collision process ($t'\to\infty$). Then, the motion equation for the advanced Green function [Eq. (10)] is integrated from $t=t'$ to $t=t_0$ with the boundary condition $G_{aa}(t',t') = i$. While in the case of the equation of motion of the F function [Eq. (9)], the integration is performed from $t=t_0$ to $t=t'$, with the boundary condition $F_{aa}(t_0,t') = [2\langle \hat{n}_a(t_0)\rangle - 1]G_{aa}(t_0,t')$.

B. Calculation of the energy level and hopping terms

The model proposed for the adiabatic atom-surface interaction can be thought as a generalization of the interaction between two atoms, where one of them consists of a system having a basis set $\{\varphi_{\mathbf{k}}\}$ (including extended valencelike and corelike band states).[18] The description is based on the symmetric orthogonalization procedure[24], in which starting from a nonorthogonal basis set $\{\varphi_a, \varphi_{\mathbf{k}}\}$ (φ_a and $\varphi_{\mathbf{k}}$ correspond to states of the isolated subsystems), the application of $(1+S)_{a\mathbf{k}}^{-1/2}$ produces the desired orthonormal basis set $\{\phi_a, \phi_{\mathbf{k}}\}$. A complete orthogonalization between the adsorbate and substrate original states is out of the question, and it is then natural to appeal to an expansion in terms of the overlap $S_{a\mathbf{k}}$. Then, by using a linear combination of atomic

orbitals (LCAO) for the substrate states and performing a mean-field approximation of the many-body interaction terms, the following expressions are found for the atom orbital energies ε_a^σ and the hopping term $V_{a\mathbf{k}}^\sigma$ (a more detailed description is given in Refs. 18 and 25):

$$\varepsilon_a^\sigma[\langle n\rangle]=\varepsilon_a^0+\tilde{U}_{aa}\langle n_{a-\sigma}\rangle-\sum_{Rs} V_{aa}^{Z_s}+\sum_{i,R_s}(\tilde{J}_{ai}\langle n_{i-\sigma}\rangle + \tilde{G}_{ai}\langle n_{i\sigma}\rangle)-\sum_{i,R_s} S_{ai}V_{ai}^{\sigma\mathrm{dim}}+\frac{1}{4}\sum_{i,R_s} S_{ai}^2\Delta E_{ai}^\sigma, \tag{12}$$

$$V_{a\mathbf{k}}^\sigma[\langle n\rangle]=\sum_{i,R_s} c_i^{\mathbf{k}}(\vec{R_s})V_{ai}^{\sigma\mathrm{dim}}[\langle n\rangle], \tag{13}$$

where now the indexes i and j run over the orbitals of the substrate atoms located at the position vector $\vec{R}_s$, $c_i^k(\vec{R_s})$ are the coefficients of the LCAO expansion of the solid $\mathbf{k}$ states, and $[\langle n\rangle]$ symbolizes the dependence of the energy level and coupling term with the occupations numbers $\langle n_{a\sigma}\rangle$ and $\langle n_{i\sigma}\rangle$. The $(\varepsilon_a^0-\Sigma_{Rs}V_{aa}^{Z_s})$ term accounts for the one electron contributions (kinetic energy and electron-nuclei interactions); $\tilde{U}_{aa}$ is the intra-atomic Coulomb repulsion term, while $\tilde{J}_{ai}$ and $\tilde{G}_{ai}$ are respectively, the direct and exchange Coulomb integrals, all them calculated by using the nonorthogonal atomic basis set and corrected by terms of order S^2. The ΔE_{ai}^σ corresponds to the difference between the projectile and surface atom energy terms. Equation (12) indicates that the atom-surface hopping is defined as a superposition of atom-atom hoppings defined only with functions orthogonalized in each dimeric space $(\vec{R},\vec{R}_s)$. $V_{ai}^{\sigma\mathrm{dim}}$ also includes the hopping contributions due to the two-electron terms within a mean-field approximation which turns it an $\langle n\rangle$-dependent coupling.

Experimental values obtained from x-ray photoemission spectroscopy data[26] are used for the core states of the solid. All the one- and two-electron atomic integrals required for the calculation are provided by a quantum chemistry code,[27] by using the Gaussian atomic orbitals given by Huzinaga.[28]

For each $\vec{R}$, the $\varepsilon_a^\sigma[\langle n\rangle]$ and $V_{ai}^{\sigma\mathrm{dim}}[\langle n\rangle]$ quantities are calculated from the adiabatic atom-surface interaction by assuming the average occupations of the projectile and surface atoms frozen at their values in the non-interacting limit. That is, $\langle n_{i\sigma}\rangle$ for the surface atoms are calculated consistently with the local density of states of the isolated surface; and $\langle n_{a\sigma}\rangle$ correspond to the initial charge-state configuration of the projectile. We adopt, for a neutral incoming projectile H^0, $\langle n_{a\uparrow}\rangle=1$, and $\langle n_{a\downarrow}\rangle=0$. When it is analyzed the H^- formation, the active state for the spinless description corresponds to the affinity level with energy $\varepsilon_a^\downarrow[\langle n\rangle]$ and hopping with the i state of the surface atom given $V_{ai}^{\downarrow\mathrm{dim}}[\langle n\rangle]$. While if it is analyzed the H^+ formation from H^0, the active state is the ionization level and the corresponding $\varepsilon_a^\uparrow[\langle n\rangle]$ and $V_{ai}^{\uparrow\mathrm{dim}}[\langle n\rangle]$ expressions must be used. The different coupling terms for each spin projection account for the different widths of the ionization and affinity levels in a self-consistent calculation.[18] This is in some way similar to the discussion by Merino *et al.*[16] about the dependence of the energy level and hopping parameters on the projectile charge configuration. However, we remark that the results arising from both models are supported by different approximations to the electronic Hamiltonian. In our case a strict mean-field treatment of the two-electron terms is carried out, and the effective one-electron coupling term is calculated consistently.

The energy level $\varepsilon_a^\sigma(\vec{R})$ obtained in this way takes into account only the short-range interactions between the projectile and the near surface atoms that are seen along its trajectory; the effect of the long-range interactions may be introduced by considering the image potential defining the behavior for large normal distances (z) to the surface ($z \geqslant z_a$). This procedure has proved to be successful in previous works.[16,18,29] In Ref. 18 the hydrogen level shift in front of an Al surface is calculated by joining the Hartree-Fock result with the correct behavior by the image potential contribution at large distances; while a pure Hartree-Fock description of the level width is proposed. A good agreement with other existing results[19] is obtained in both cases. The energy level as a function of the projectile-surface distance $\vec{R}$ is then proposed as

$$E_a^\sigma(\vec{R})=\begin{cases}\varepsilon_a^\sigma(\vec{R})-\varepsilon_a^\sigma(\vec{R}_a)+\varepsilon_\infty^\sigma+V_{im}(z_a) & \text{for } z<z_a\\ \varepsilon_\infty^\sigma+V_{im}(z) & \text{for } z\geqslant z_a\,.\end{cases} \tag{14}$$

In the case of H^- formation $\varepsilon_\infty^\downarrow=-0.75$ eV and $V_{im}(z)=-1/4(z-z_0)$; while for H^+ formation $\varepsilon_\infty^\uparrow=-13.6$ eV and $V_{im}(z)=1/4(z-z_0)$. Here z is the normal component to the surface, and $z_0=3.06$ a.u. is the image plane position for the Al (100) surface. The z_a distance is assumed equal to 8 a.u. as in Ref 18. In this form the energy level obtained within a mean field calculation has been shifted to join in a smooth way with the correct asymptotic behavior that includes the effect of the long-range interactions. As it is known, the closed shell structure used for describing the H^- ion does not correspond to a bound state, then the $-\varepsilon_a^\sigma(\vec{R}_a)+\varepsilon_\infty^\sigma$ term is introduced to account for the correct value of the affinity level.

Related with the dynamical aspects of the charge transfer process we have that the atom's wave function (φ_a') as seen from the surface's reference frame has the following asymptotic behavior $(\vec{R}\to\infty)$:

$$\varphi_a'(\vec{r},t)=\exp(i\vec{v}.\vec{r})\varphi_a(\vec{r}-\vec{R}(t))\times\exp\{-i[E_a^\sigma(\vec{R})+v^2/2]t\},$$

where $\varphi_a(\vec{r}-\vec{R}(t))$ is the static wave function and $\vec{v}$ is the projectile velocity. The Galilean transformation phases or electron-translation factor[30] should be included in the calculation of energy level and hopping terms for a more appropriate description of the charge exchange. To calculate velocity-dependent hopping terms by including the phase factor $\exp(i\vec{v}.\vec{r})$ means a formidable task. Taking into ac-

count the rather low nuclear velocities ($v \ll 1$ a.u.) as compared with the electron velocity in the H-1s orbital considered in the calculation, we calculate the atomic hopping intergrals by considering $v=0$. This can be assumed as a crude first order approximation. Therefore, we keep the effect of the Galilean transformation only in the shift of the atomic energy level as seen from the surface:

$$E_a^\sigma[\vec{R}(t)] \rightarrow E_a^\sigma(\vec{R}(t)) + v^2/2. \tag{15}$$

The usual treatment of the parallel velocity effect through the shift in the electron Fermi distribution as seen from the rest frame on the moving atom is only strictly valid for very grazing collisions.[12] This is not applicable to our description that focuses the opposite limit: the surface as the rest frame, and the close encounters between projectile and target atoms playing an important role in the collisional process.

C. Self-energies and projectile's trajectory

Turning back to expressions (8) and (11) for the self-energies and using the expansion LCAO [Eq. (13)] for the hopping term V_{ak}^σ, we can write

$$\Sigma_X^r(t,\tau) = -i\Theta(t-\tau) \times \sum_{i,j,R_s,R_s'} V_{ai}^{\dim}[\vec{R}(t)-\vec{R}_s] V_{ja}^{\dim}[\vec{R}(\tau)-\vec{R}'_s] \times \int_{-\infty}^{\infty} d\epsilon \rho_{i,j,R_s,R_s'}(\epsilon) \exp[i\epsilon(t-\tau)], \tag{16}$$

$$\Omega_X(t,\tau) = i \sum_{i,j,R_s,R_s'} V_{ai}^{\dim}[\vec{R}(t)-\vec{R}_s] \times V_{ja}^{\dim}[\vec{R}(\tau)-\vec{R'}_s] \times \int_{-\infty}^{\infty} d\epsilon [2f_<(\epsilon)-1] \rho_{i,j,R_s,R_s'}(\epsilon) \times \exp[i\epsilon(t-\tau)], \tag{17}$$

where $\rho_{i,j,R_s,R_s'}(\epsilon)$ is given by the expression

$$\rho_{i,j,R_s,R_s'}(\epsilon) = \sum_{\mathbf{k}} c_i^{\mathbf{k}*}(\vec{R}_s) c_j^{\mathbf{k}}(\vec{R'}_s) \delta(\epsilon-\epsilon_{\mathbf{k}}),$$

and $f_<(\epsilon)$ is the Fermi-Dirac distribution [$\Theta(\epsilon-\epsilon_F)$ for $0K$ temperature]. In the calculation of expressions (16) and (17) only the diagonal terms in $\vec{R}_s$, and $\vec{R'}_s$ ($\vec{R}_s=\vec{R'}_s$) are maintained by assuming that they provide the main contribution. The Al core-bands are considered as localized states, then $\rho_{i,j,R_s,R_s}(\epsilon) = \Sigma_c \delta_{ic}\delta_{jc}\delta(\epsilon-\epsilon_c)$. The local and partial density of valence states $\rho_{i,j,R_s,R_s}(\epsilon)$ for the Al(100) surface is calculated projecting the semiinfinite crystal onto three or four metallic surface layers through a decimation technique.[31]

In Fig. 1 we show schematically the trajectory used in this work. The trajectory is assumed to occur in the $x-z$ plane,

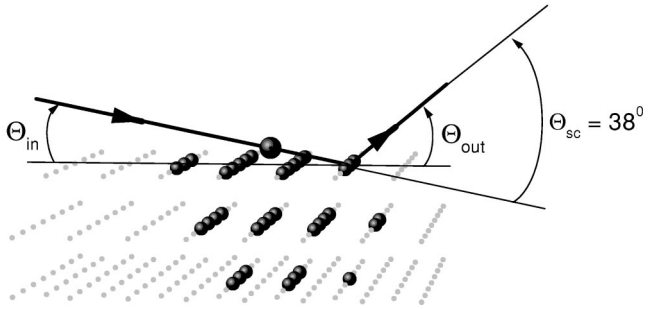

FIG. 1. Schematic view of the (classical) trajectory of a projectile colliding with a crystalline surface. The big circles correspond to atoms inside the near- neighbor sphere centered at the projectile position which are operative in the calculation. The incident and exit angles, and also the scattering angle, are indicated.

and a row of Al atoms is along the x direction. The distances of closest approach ($R_{\min}$) for the different incoming energies are obtained from the interaction energy between H and Al atoms, their values being 0.15, 0.09, and 0.04 a.u. for 1, 2, and 4 keV, respectively. The ($x_{\min}$,$z_{\min}$) coordinates of $\vec{R}_{\min}$ are calculated by using the usual concepts of the theory of collision in a central field[32] (the laboratory frame is assumed to be coincident with the center of mass system in this case). Thus

$$x_{\min} = -R_{\min}\cos(\Phi+\Theta_{in}),$$

$$z_{\min} = R_{\min}\sin(\Phi+\Theta_{in}),$$

where $\Phi=(\pi-\Theta_{sc})/2$, Θ_{sc} being the scattering angle and Θ_{in} the incident angle measured with respect to the surface. A more general approach would be to average over many trajectories with y coordinates inside a surface unit cell. On the other hand, the single scattering picture is supported by the experimental evidence that there is a very small effect of trajectories corresponding to particles having penetrated and suffered multiple collisions.[13,14]

III. RESULTS AND DISCUSSION

In Fig. 2 we show the projectile affinity level as a function of the normal distance z to the surface (the negative values of z only indicate the incoming trajectory, and the Al Fermi level defines the zero value for the energies). The case in this figure corresponds to an incident angle respect to the surface equal to 30°, therefore the exit angle is 8°. Different contributions to the level shift are considered: (i) only the short-range interactions [Eq. (12)] (TRAJ calculation), (ii) the short-range interactions plus the image potential [Eq. (14)] (IP calculation), and (iii) the complete calculation also including the kinetic energy term due to the projectile nucleus motion Eq. (15) (TF+ IP calculation). The structure observed in the energy level is produced by the change in the set of surface atoms that are being operative in the interaction with the projectile along its trajectory. This means that the projectile atom ''sees'' different surface atoms depending on its position along the trajectory. This structure is then more pronounced the smaller the angle between the trajec-

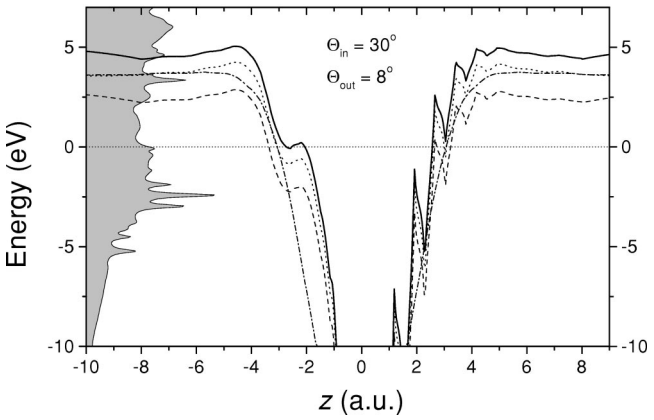

FIG. 2. The affinity level as a function of the normal distance to the surface. Negative (positive) values for z correspond to the incoming (outgoing) trajectory. Solid line: TF+IP calculation. Dashed line: IP calculation. Dotted line: TRAJ calculation. Dash-dotted line: on top calculation. We also include the Al(100) density of states used in the calculation. The energy zero is defined at the Al Fermi level.

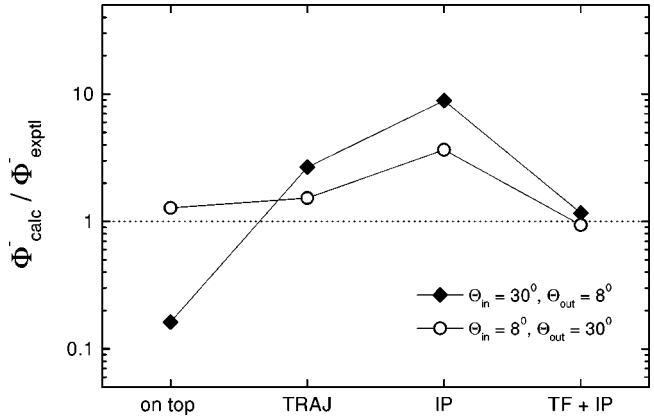

FIG. 3. Ratio between the theoretical and experimental ion fractions for different options of calculation. Circles: $\Theta_{in}=8°$ and $\Theta_{out}=30°$. Diamonds: $\Theta_{in}=30°$ and $\Theta_{out}=8°$. The incoming kinetic energy is 4 keV.

tory and the surface is. For distances $z \geqslant 5$ a.u., a smooth variation of the affinity level is obtained. Therefore, the level shift is determined by the localized atom-atom interactions in the close distance region, while it is defined by the surface as an extended system in the long distance region. To our knowledge, this is the first time that such a detailed information is included in the calculation of the energy level shift. It is also shown in this figure the energy level calculated by considering a normal trajectory with respect to the surface, being the short-range interactions with only the scatterer atom at the surface determining the variation of the affinity level in this case (dash-dotted line). This on-top calculation represents the roughest approximation to the present collisional system.

The same negative ion fractions are obtained by using either H^0 or H^- as initial conditions in all the cases. This fact together with the same negative ion fractions measured with either positive or negative hydrogen beams,[13,14] allow one to conclude that a practically total conversion to H^0 is occurring in the incoming trajectory due to the very efficient resonant mechanism opened at large distances.

The ratio between the calculated negative ion fraction and the experimental value obtained by Maazaouz and co-workers.[13,14] is shown in Fig. 3 for the three different options of the affinity level (TRAJ, IP, and IP+TF). The incident kinetic energy equal to 4 keV and two scattering geometries, $\Theta_{in(out)}=30°$ (8°) and $\Theta_{in(out)}=8°(30°)$, are analyzed in this figure. It is also included the on-top calculation corresponding to the normal scattering ($\Theta=90°$), where the information about the actual trajectory enters only through the correct normal component of the velocity ($v_{in(out)}=v^* \sin\Theta_{in(out)}$). The dispersion among the different calculations is expected to be more pronounced as closer to the surface the ion trajectory is. In Fig. 3 this is observed for the smallest Θ_{out}, suggesting that the ion fractions are being defined in the outgoing trajectory. The difference between the on-top and TRAJ calculations is basically provided by the effect of the localized interactions with many near surface atoms that the second option introduces in the mean-field calculation of energy and hopping terms. As seen from Fig. 2, this is evidenced by a marked structure in the energy level variation with the distance to the surface in the case of small angles. The effect of the long-range interactions through the level shift by the image potential is expected to be more important as the time the projectile spends far from the surface is longer, and this is the case of trajectories with small angles. Figure 3 shows that the values of Θ_{out} interest fundamentally to determine this effective time. Finally, when the three ingredients are taken into account in the level shift description (short-range interactions with the near surface atoms, the long range-interaction, and the motion of the pro-

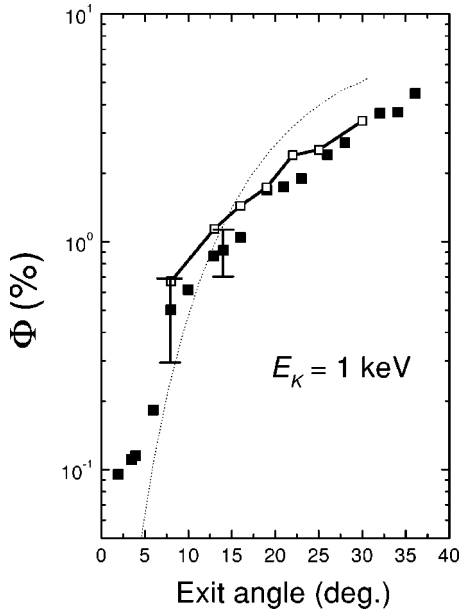

FIG. 4. Negative ion fraction as a function of the exit angle for an incoming energy $E_k=1$ keV. Solid squares: experimental data from Ref. 13. Open square: this calculation. Dotted line: CAM results from Ref. 13.

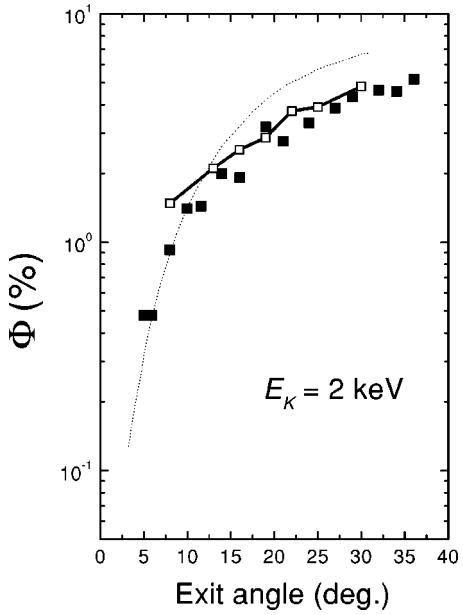

FIG. 5. The same as in Fig. 4 for $E_k = 2$ keV. Experimental data and CAM results extracted from Ref. 14.

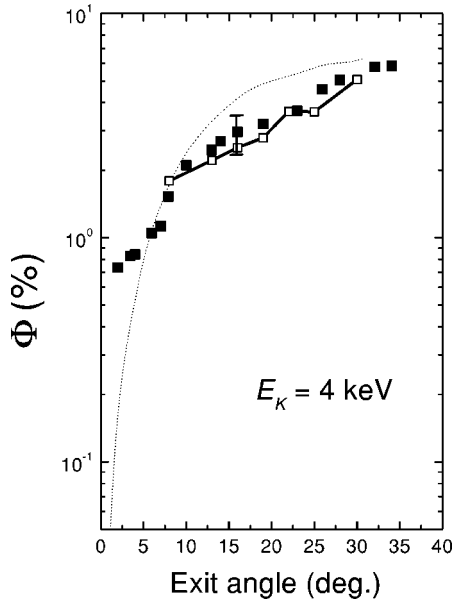

FIG. 6. The same as in Fig. 4 for $E_k = 4$ keV.

jectile relative to the reference frame on the surface) (the hopping terms are always calculated within the mean-field approximation), an excellent agreement with the experimental result is obtained. This agreement is in the same way achieved for the three incoming energies and for all the scattering geometries analyzed, as it can be seen from Figs. 4, 5, and 6. Compared with the theoretical results from the CAM method, the full quantum calculation along the whole trajectory accounts for the correct charge state of the hydrogen atom near the surface, and a better description in the region of more violent collisions (large values of Θ_{out}) is obtained. Some apparent structure is observed in the dependence of the calculated ion fraction with the exit angle around $\Theta_{out} \approx 22°$ for the three incoming energies analyzed. The origin may be due to the atomic surface roughness seen by the projectile together with the amplitude interferences between the in and out trajectories of rather large and similar angles.

IV. CONCLUSIONS

The present calculation of the hydrogen atom collision against an Al surface includes the most detailed description up to this moment of the atom-surface interaction within a quantum mechanical treatment of the time-dependent process. The scattering geometry is taken into account by considering a binary collision determining the trajectory, but the inelastic processes involve the interaction with all the surface atoms that are operative along the projectile trajectory. The level shift of the incoming atom is calculated by considering the short-range interactions well treated by a mean-field approximation, the long-range interaction through the image potential, and the energy shift due to the atom motion respect to the surface reference frame. Both, the extended nature of the surface through the local and partial density of states, and the localized atom-atom hopping integrals calculated within a mean-field approximation, define the atom-surface hopping terms. It is found that no matter the initial projectile charge is, a total conversion to neutral hydrogen occurs in the incoming trajectory due to a very efficient resonant mechanism; and the negative ion formation by the same mechanism is mainly defined in the outgoing path. An excellent agreement with the experimental results is obtained for three different values of the incoming energy and a wide range of exit angles.

ACKNOWLEDGMENTS

This work was supported by Grants (PIP) No. 4799/97 from Consejo Nacional de Investigaciones Científicas y Tecnológicas (CONICET), (CAI+D) No. 6-1-76 from Universidad Nacional del Litoral (UNL) and 14022-27 from Fundación Antorchas, Argentina. E.C.G. and P.G.B. were partially supported by CONICET.

[1] R. Souda, T. Aizawa, C. Oshima, S. Otani, and Y. Ishizawa, Phys. Rev. B **40**, 4119 (1989).

[2] R. Souda, T. Aizawa, W. Hayami, S. Otani, and Y. Ishizawa, Phys. Rev. B **42**, 7761 (1990).

[3] R. Souda, W. Hayami, T. Aizawa, and Y. Ishizawa, Phys. Rev. B **43**, 10 062 (1991).

[4] R. Souda, K. Yamamoto, W. Hayami, T. Aizawa, and Y. Ishizawa, Phys. Rev. B **51**, 4463 (1995).

[5] R. Souda, T. Suzuki, and K. Yamamoto, Surf. Sci. **397**, 63 (1998).

[6] Evelina A. García, P. G. Bolcatto, and E. C. Goldberg, Phys. Rev. B **52**, 16 924 (1995).

[7] Evelina A. García, and E. C. Goldberg, Phys. Rev. B **57**, 6672

(1998).
[8] Evelina A. García, P. G. Bolcatto, M. C. G. Passeggi, and E. C. Goldberg, Phys. Rev. B **59**, 13 370 (1999).
[9] F. Wyputta, R. Zimny, and H. Winter, Nucl. Instrum. Methods Phys. Res. B **58**, 379 (1991).
[10] H. Nienhaus, R. Zimny, and H. Winter, Radiat. Eff. Defects Solids **109**, 1 (1989).
[11] R. Zimny, H. Nienhaus, and H. Winter, Nucl. Instrum. Methods Phys. Res. B **48**, 361 (1990).
[12] A. G. Borisov, D. Teillet-Billy, and J. P. Gauyacq, Phys. Rev. Lett. **68**, 2842 (1991); Surf. Sci. **278**, 99 (1992).
[13] M. Maazouz, R. Baragiola, A. Borisov, V. A. Esaulov, S. Lacombe, J. P. Gauyacq, L. Guillemot, and D. Teillet-Billy, Surf. Sci. **364**, L568 (1996).
[14] M. Maazouz, A. G. Borisov, V. A. Esaulov, J. P. Gauyacq, L. Guillemot, S. Lacombe, and D. Teillet-Billy, Phys. Rev. B **55**, 13 869 (1997).
[15] J. Merino, N. Lorente, F. Flores, and M. Yu Gusev, Nucl. Instrum. Methods Phys. Res. B **125**, 250 (1997); N. Lorente, J. Merino, F. Flores, and M. Yu Gusev, *ibid.* **125**, 277 (1997).
[16] J. Merino, N. Lorente, P. Pou, and F. Flores, Phys. Rev. B **54**, 10 959 (1996).
[17] J. Merino, N. Lorente, M. Yu. Gusev, F. Flores, M. Maazouz, L. Guillemot, and V. A. Esaulov, Phys. Rev. B **57**, 1947 (1998).
[18] P. G. Bolcatto, E. C. Goldberg, and M. C. G. Passeggi, Phys. Rev. B **58**, 5007 (1998).
[19] A. G. Borisov, D. Teillet-Billy, and J. P. Gauyacq, Nucl. Instrum. Methods Phys. Res. B **78**, 49 (1993); P. Nordlander, and J. C. Tully, Phys. Rev. Lett. **61**, 990 (1988); S. A. Deutscher, X. Yang, and J. Burgdöfer, Phys. Rev. A **55**, 466 (1997).
[20] L. V. Keldysh, Zh. Éksp. Teor. Fiz. **47**, 1515 (1964) [Sov. Phys. JETP **20**, 1018 (1965)].
[21] R. Zimny, Surf. Sci. **233**, 333 (1990).
[22] D. C. Langreth and P. Nordlander, Phys. Rev. B **43**, 2541 (1991).
[23] E. C. Goldberg, E. R. Gagliano, and M. C. G. Passeggi, Phys. Rev. B **32**, 4375 (1985).
[24] P. O. Lowdin, J. Chem. Phys. **18**, 365 (1950).
[25] P. G. Bolcatto, E. C. Goldberg, and M. C. G. Passeggi, Phys. Rev. A **50**, 4643 (1994); J. O. Lugo, L. I. Vergara, P. G. Bolcatto, and E. C. Goldberg, *ibid.* **65**, 022503 (2002).
[26] J. A. Bearden and A. F. Burr, Rev. Mod. Phys. **39**, 125 (1967).
[27] This calculation was performed using the commercial program GAUSSIAN98.
[28] S. Huzinaga, J. Chem. Phys. **42**, 1293 (1965); S. Huzinaga, J. Andzelm, M. Klobukowski, E. Radzio-Andzelm, Y. Sakai, and H. Tatewaki, in *Gaussian Basis Set for Molecular Calculations*, edited by S. Huzinaga (Elsevier, Amsterdam, 1984).
[29] P. G. Bolcatto, Ph. D. thesis, Universidad Nacional de Rosario, Argentina, 1997.
[30] J. B. Delos, Phys. Rev. A **23**, 2301 (1981).
[31] F. Guinea, C. Tejedor, F. Flores, and E. Louis, Phys. Rev. B **28**, 4397 (1983).
[32] H. Goldstein, *Classical Mechanics* (Addison-Wesley, Reading, MA 1959).